Background Matters: A Correction Scheme for Dynamic Iterative CBCT with Limited Grid Size

Oliver Taubmann*†, Günter Lauritsch‡, Gregor Krings§, and Andreas Maier*†
*Pattern Recognition Lab, Friedrich-Alexander-University Erlangen-Nuremberg, Germany
†Graduate School in Advanced Optical Technologies (SAOT), Erlangen, Germany
‡Siemens Healthcare GmbH, Forchheim, Germany
§University Medical Center Utrecht, Netherlands

***Abstract*—Dynamic cone-beam computed tomography (CBCT) imaging of the thorax, i. e. time-resolved reconstruction w. r. t. cardiac or respiratory motion, requires sophisticated algorithms, many of which are iterative and computationally expensive in terms of both runtime and memory. For the latter, hardware constraints pose a considerable challenge insofar as the volume grid cannot be chosen arbitrarily large. On the other hand, choosing a small grid may lead to severe artifacts if the object exceeds the size of the reconstruction domain. Additionally, lateral truncation of the projection data is commonly encountered as, e. g., flat panel detectors employed in interventional C-arm devices are not large enough to simultaneously image the entire width of the thorax in most patients. In iterative reconstruction, mild data truncation artifacts can also be alleviated by reconstructing on a sufficiently large grid. We present a simple model to incorporate information from outside the target grid in dynamic reconstruction. Its main component is the reconstruction of a static background image used to precompute an additive data correction term, which can be used in combination with any dynamic iterative reconstruction method. The effectiveness of our approach is demonstrated in a numerical phantom and clinical patient data.**

I. Introduction

Challenging dynamic imaging tasks, such as the generation of time-resolved cardiac volume series from rotational angiography sequences [1], often require the incorporation of regularizers and the use of sophisticated optimization methods for iterative reconstruction. Therefore, such methods can have memory footprints in the range of several times the size of the unknown images. Also, many iterations may be required to converge to a desirable solution.

Considering hardware limitations and the huge computational cost involved, it frequently proves prohibitive to employ a reconstruction grid (volume of interest, VOI) that is large enough to encompass the whole object [2]. Choosing a smaller grid typically causes no harm for analytical reconstruction methods such as filtered backprojection, where each voxel is obtained independently from the others. However, it is critical for algebraic, iterative methods which rely on repeated forward-projections of intermediate image estimates.

One potential way of reducing the computational demand associated with reconstructing larger volumes is the use of irregular grids with non-uniform resolution [2], which necessitate a dedicated implementation of the projection operators.

Another type of truncation is lateral truncation of the projection data [3]. In terms of reconstruction, it means that the imaged object extends outside the reconstruction field of view (FOV), i. e. outside the area that is observed from all angulations. This is often the case when imaging the torso, which is also the relevant anatomic region for dynamic cardiac and respiratory imaging tasks. It causes artifacts inside the FOV as Radon inversion is a non-local operation [4], [5].

Many methods have been proposed to cope with this type of truncation [6], [7]; the majority is based on sophisticated projection data extrapolation models [4], [8], [9]. In iterative reconstruction, enlarging the grid size can also help to alleviate truncation-related artifacts [2].

In this paper, we propose a straight-forward correction scheme tailored to dynamic imaging that relies on a background estimate reconstructed on a large grid using a simple, static reconstruction method. We show that the resulting correction term can be computed prior to the dynamic reconstruction, and is thus independent thereof. It is incorporated by merely correcting the projection data, i. e. in a manner such that the dynamic reconstruction algorithm need not be modified. We demonstrate the effectiveness of our approach in a phantom and a clinical data set.

II. Materials and Methods

A. Background-Based Correction

In order to minimize artifacts in iterative reconstruction, it is advisable to employ an image grid that is larger than the desired VOI [2]. Our method is based on two simplifying model assumptions:

- **(i)** For dynamic imaging, the region outside the VOI (*background*) is assumed to be static. This requires differences between the motion states to be negligible w. r. t. their aptitude for reducing truncation artifacts inside the VOI.
- **(ii)** The background obtained in a static reconstruction from all data is comparable to the assumedly static background (see **(i)**) obtained in a dynamic reconstruction. Therefore, the background can be precomputed.

The correction scheme derived from these assumptions comprises the following steps, illustrated in Fig. 1. Please note that for convenience of notation, the symbols for images and projection data introduced below denote their vectorized representations.

DOI: 10.12059/Fully3D.2017-11-3202032

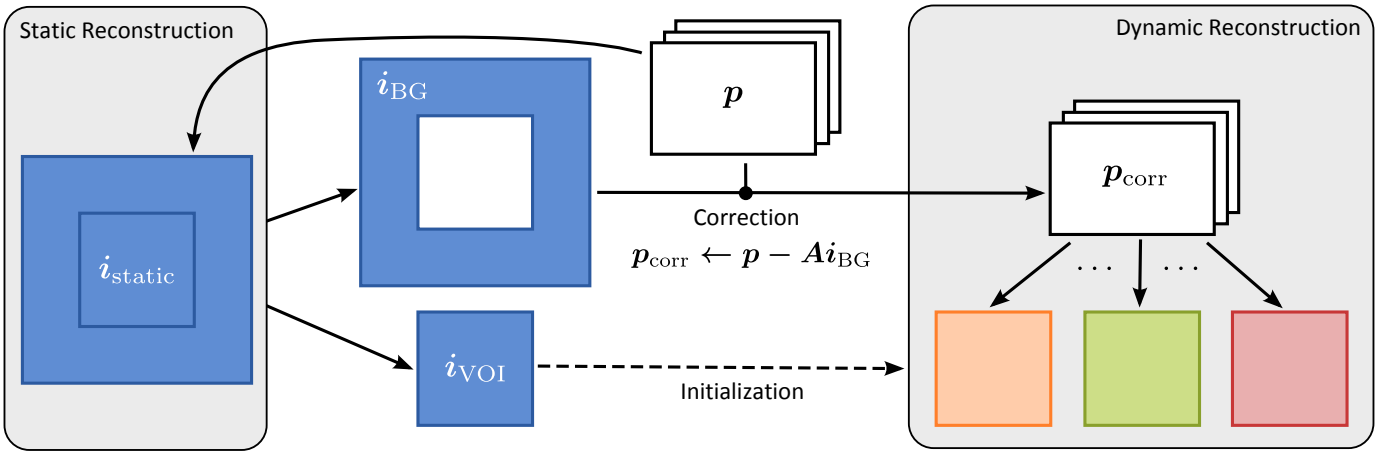

Fig. 1: A schematic overview of the proposed approach. A static background is estimated to correct the projection data prior to dynamic reconstruction. In practice, the conceptually empty interior of I_{BG} is filled with zero values.

(a) Using any conventional algorithm, reconstruct a (motion-corrupted) static image i_{static} from all available projection data p on a grid larger than the VOI.

(b) Separate the reconstructed image into two images: i_{VOI}, the part of the image corresponding to the VOI to reconstruct dynamically later, and i_{BG}, which corresponds to the background. Images i_{VOI} and i_{BG} can easily be obtained by cropping i_{static} and zeroing the cropped region in the original (uncropped) i_{static}, respectively.

(c) Perform a dynamic iterative reconstruction on the desired VOI grid. If applicable, initialize the optimization with copies of i_{VOI} for all motion states. In the forward projection step, incorporate the background: Instead of computing the residual error as $Ai - p$, where A is the projection operator (system matrix) and i the current image estimate, we compute $A(i + i_{\text{BG}}) - p$, which can be rewritten as,

$$\overbrace{A(i + i_{\text{BG}}) - p}^{\text{Residual error}} = \tag{1}$$

$$= Ai + Ai_{\text{BG}} - p = \tag{2}$$

$$= Ai - \underbrace{(p - Ai_{\text{BG}})}_{\text{Corrected data } p_{\text{corr}}} . \tag{3}$$

This means that we can precompute corrected projection data p_{corr} and use it for the dynamic reconstruction instead of the original p. The backprojection step is not modified either; it only updates the VOI since we are no longer operating on a larger grid and the background is assumed to be static.

Regarding efficiency, we note that step **(b)** is negligible compared to the actual reconstruction tasks and step **(c)** remains exactly as fast as before apart from a single forward projection and subtraction to perform the correction. Only step **(a)** introduces perceptible overhead. However, it is moderate because a rough estimate of the background may suffice, which, in the case of iterative algorithms, means that only very few iterations are needed. It is also independent of the number of motion states to be reconstructed dynamically.

B. Data

We evaluate our approach on CBCT of cardiac chambers.

Phantom: For validation, we use a dynamic numerical phantom based on XCAT [10], of which we generate projections [11] using the trajectory of a real C-arm device. Exemplary frames from the simulated data are shown in Fig. 2. The acquisition protocol consists of 133 projection images captured with an angular increment of 1.5°. The isotropic pixel resolution is 0.31 mm/pixel (0.21 mm/pixel in isocenter), the detector size 960×960 pixels. The whole scan covers 12 heart cycles and we jointly reconstruct 8 equally distributed cardiac phases. For each individual phase, 12 projection images are

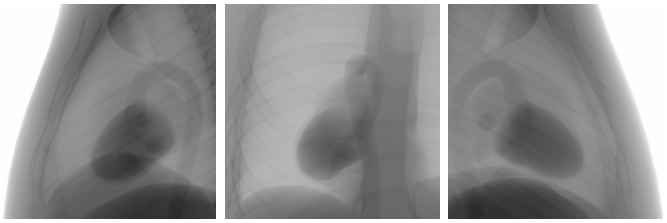

(a) Frame 1 (b) Frame 70 (c) Frame 133

Fig. 2: Projections from the simulated phantom data set.

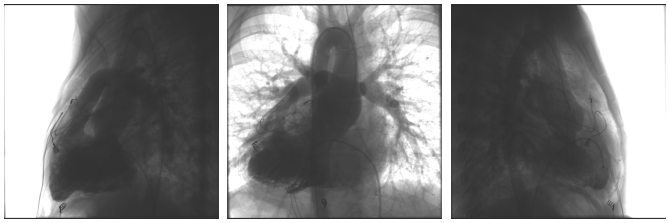

(a) Frame 20 (b) Frame 70 (c) Frame 128

Fig. 3: Projections from the clinical patient data set.

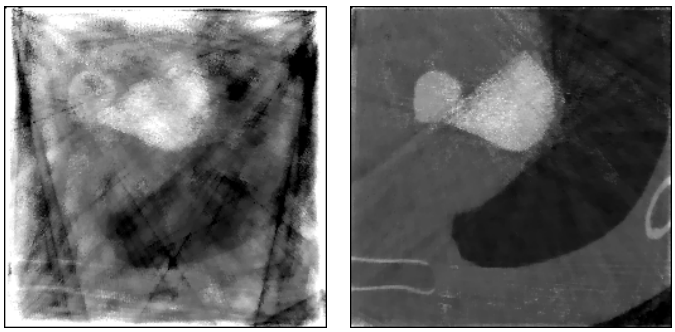

(a) Uncorrected (b) Corrected

Fig. 4: Results for the *VOI-limited* case (phantom). The grayscale window is $[-1000, 970]$ HU.

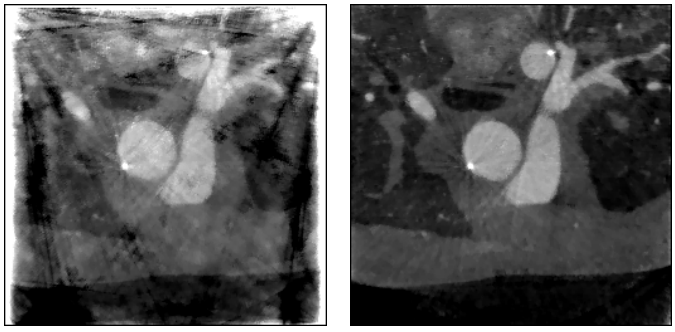

(a) Uncorrected (b) Corrected

Fig. 5: Results for the *VOI-limited* case (clinical data). The grayscale window is $[-1000, 1810]$ HU.

used in total by selecting only the best-fitting one from each cycle. While more severe data truncation could be simulated, we chose this setup because it reflects a realistic amount of truncation as it is typically encountered in cardiac C-arm CT.

Clinical Data: We also demonstrate our method in a clinical patient data set acquired with an Artis zee biplane (Siemens Healthcare GmbH, Forchheim, Germany). Exemplary frames from this data set are shown in Fig. 3. The acquisition protocol is identical to the one described for the phantom data set above. The scan covers 14 heart cycles and we again reconstruct 8 phases.

C. Experimental Setup

We employ a spatially and temporally total-variation-regularized iterative method for 4-D reconstruction [12]. Two setups are compared:

Uncorrected: Static reconstruction on a 256^3 grid (20 gradient descent iterations) to initialize, followed by dynamic reconstruction of 8 motion states (180 4-D iterations).

Corrected: Static reconstruction to initialize as above, but on a 512^3 grid, followed by the described correction step and, subsequently, dynamic reconstruction as above.

We also discriminate between the following two cases:

VOI-limited: The reconstructed VOI is smaller than the FOV, i. e., the limiting factor is the truncation of the reconstruction grid. This is the case when we choose an isotropic voxel size of $0.5\,\text{mm}$ for the 256^3 grid.

FOV-limited: The reconstructed VOI is large enough to contain the FOV, but the object does not fit the detector, i. e., the limiting factor is the truncation of the projection data. For our data, this is the case when we choose an isotropic voxel size of $1\,\text{mm}$ for the 256^3 grid.

III. Results and Discussion

Phantom: In the VOI-limited case (Fig. 4), when no correction is performed, image quality is degraded to the point where the object is almost completely obscured by artifacts (Fig. 4a). In contrast, the corrected version (Fig. 4b) recovers the anatomy very well, barring some streaks and errors close to the grid boundaries. The key cause of the artifacts in Fig. 4a is the excess amount of object mass that is observed in the projections, but cannot be explained consistently within the limited view of the reconstruction domain. The correction essentially removes this surplus mass, allowing for a more stable reconstruction. Quantitatively, the difference corresponds to an increase of the correlation coefficient with the ground truth from 19.1% (Fig. 4a) to 93.5% (Fig. 4b).

The results for the FOV-limited case are shown in Fig. 6. In the uncorrected image (Fig. 6a), mild cupping artifacts are observed. The borders of the FOV appear brighter than they are supposed to, particularly at the top and left boundaries where the object would extend further. This effect, which also becomes apparent in the line profile plotted in Fig. 6d, is reduced considerably in the corrected image (Fig. 6b). Additionally, the image exhibits less streaking, rendering it more similar to the ground truth (Fig. 6c) than the uncorrected variant. In terms of correlation, this is an improvement from 96.4% (Fig. 6a) to 97.3% (Fig. 6b). The change is comparatively small as the artifacts in question have a low amplitude in relation to the image content.

Clinical Data: The results obtained for the clinical data set closely mirror those of the phantom study. For the VOI-limited case (Fig. 5), a proper reconstruction of the object is only achieved with the corrected version, similar to the result in Fig. 4. The FOV-limited case is shown in Fig. 7. While no ground truth is available here, the difference between the uncorrected and corrected versions reveals a low-frequency bias, especially in the posterior region, and some streak artifacts that are no longer present after correction.

IV. Conclusion

We presented a simple and efficient approach to incorporating information from outside the target volume in dynamic iterative reconstruction of CBCT data. Its main advantage lies in its universality; based solely on a precomputable correction, it can readily be applied to any dynamic reconstruction algorithm. In experiments on 4-D cardiac C-arm CT reconstruction of phantom and clinical data, it proved beneficial for both considered cases: When the reconstruction grid is smaller than the reconstruction FOV as well as when the projection data is moderately truncated. Our findings also underline the

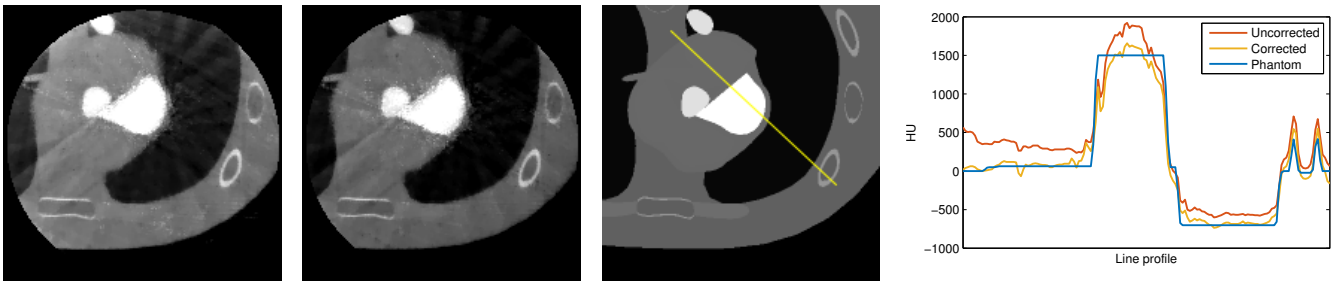

(a) Uncorrected (b) Corrected (c) Phantom (d) Line profiles

Fig. 6: Results for the *FOV-limited* case (a, b). For comparison, a corresponding rasterization of the phantom is shown in (c). The yellow line indicates the location of the intensity profiles plotted in (d). The grayscale window is $[-1000, 1250]$ HU.

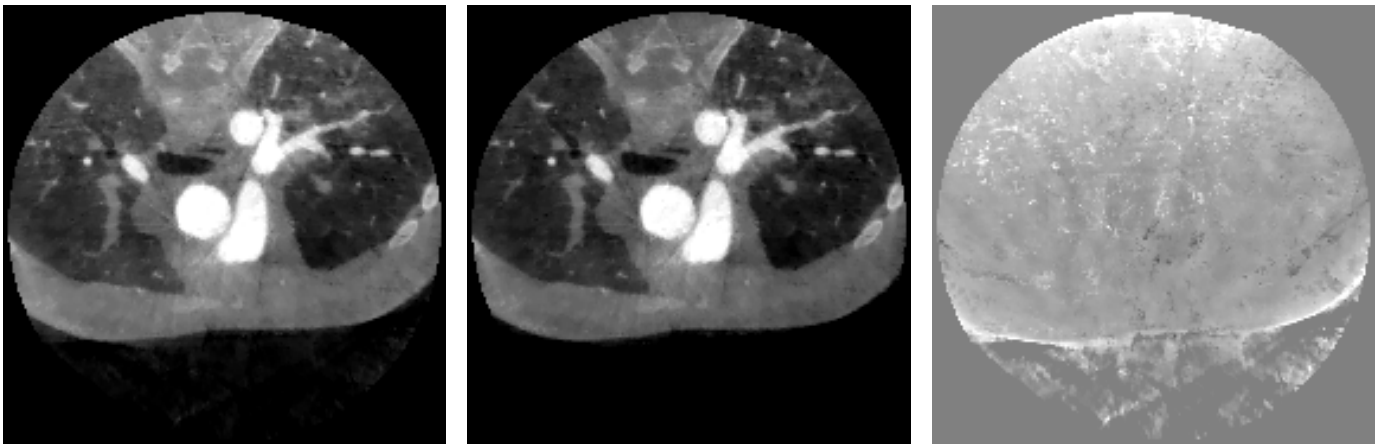

(a) Uncorrected (b) Corrected (c) Difference

Fig. 7: Results for the *FOV-limited* case (clinical data). The grayscale window is $[-1000, 2370]$ HU for (a, b) and $[-560, 560]$ HU for the difference image (c).

general importance of using sufficiently large grids in iterative reconstruction.

Future work could seek to determine ideal background sizes to achieve an optimal trade-off between computational cost and performance of artifact reduction.

Acknowledgments and Disclaimer: The concepts and information presented in this paper are based on research and are not commercially available.

REFERENCES

[1] C. Mory, V. Auvray, B. Zhang, M. Grass, D. Schäfer, S. Chen, J. Carroll, S. Rit, F. Peyrin, P. Douek, and L. Boussel, "Cardiac C-arm computed tomography using a 3D + time ROI reconstruction method with spatial and temporal regularization," *Med Phys*, vol. 41, p. 021903, 2014.

[2] S. Rit, M. van Herk, and J.-J. Sonke, "Fast distance-driven projection and truncation management for iterative cone-beam CT reconstruction," in *Fully3D*, Beijing, China, 2009, p. 49–52.

[3] Y. Xia, H. Hofmann, F. Dennerlein, K. Müller, C. Schwemmer, S. Bauer, G. Chintalapani, P. Chinnadurai, J. Hornegger, and A. Maier, "Towards Clinical Application of a Laplace Operator-based Region of Interest Reconstruction Algorithm in C-arm CT," *IEEE Trans Med Imaging*, vol. 33, no. 3, pp. 593–606, 2014.

[4] R. Chityala, K. R. Hoffmann, S. Rudin, and D. R. Bednarek, "Artifact reduction in truncated CT using sinogram completion," in *SPIE Med Imag*, 2005, pp. 2110–2117.

[5] F. Dennerlein and A. Maier, "Region-of-interest reconstruction on medical C-arms with the ATRACT algorithm," in *SPIE Med Imag*, 2012, p. 83131B.

[6] B. Zhang and G. L. Zeng, "Two-dimensional iterative region-of-interest (ROI) reconstruction from truncated projection data," *Med Phys*, vol. 34, no. 3, pp. 935–944, 2007.

[7] P. T. Lauzier, J. Tang, and G.-H. Chen, "Time-resolved cardiac interventional cone-beam CT reconstruction from fully truncated projections using the prior image constrained compressed sensing (PICCS) algorithm," *Phys Med Biol*, vol. 57, no. 9, p. 2461, 2012.

[8] D. Kolditz, M. Meyer, Y. Kyriakou, and W. A. Kalender, "Comparison of extended field-of-view reconstructions in C-arm flat-detector CT using patient size, shape or attenuation information," *Phys Med Biol*, vol. 56, no. 1, p. 39, 2011.

[9] Y. Xia, S. Bauer, A. Maier, M. Berger, and J. Hornegger, "Patient-bounded extrapolation using low-dose priors for volume-of-interest imaging in C-arm CT," *Med Phys*, vol. 42, no. 4, pp. 1787–1796, 2015.

[10] W. P. Segars, G. Sturgeon, S. Mendonca, J. Grimes, and B. M. W. Tsui, "4D XCAT phantom for multimodality imaging research," *Med Phys*, vol. 37, pp. 4902–4915, 2010.

[11] A. Maier, H. Hofmann, C. Schwemmer, J. Hornegger, A. Keil, and R. Fahrig, "Fast Simulation of X-ray Projections of Spline-based Surfaces using an Append Buffer," *Phys Med Biol*, vol. 57, no. 19, pp. 6193–6210, 2012.

[12] O. Taubmann, V. Haase, G. Lauritsch, Y. Zheng, G. Krings, J. Hornegger, and A. Maier, "Assessing cardiac function from total-variation-regularized 4-D C-arm CT in the presence of angular undersampling," *Phys Med Biol*, vol. 62, no. 7, p. 2762, 2017.